

# Radial characterization of wave magnetic field components during helicon discharge in a small aspect ratio torus

MANASH KUMAR PAUL<sup>†</sup> and DHIRAJ BORA

Institute for Plasma Research, Bhat, Gandhinagar 382428, India  
(manashkr@gmail.com)

(Received 17 February 2009 and accepted 5 March 2009, first published online  
15 April 2009)

**Abstract.** Wave magnetic field components are measured across the radius ( $-10 \text{ cm} \leq r \leq 10 \text{ cm}$ ) for a low-pressure (0.3 mbar) helicon discharge, in a toroidal vacuum chamber of small aspect ratio. Radial variation of the wave magnetic field components, measured during the helicon mode of the discharge, exhibit strong poloidal asymmetry which contribute significantly to the wave-induced helicity. The rise in the magnitude of the radial electric field with radiofrequency power, observed during discharge mode transition, supports better radial confinement of the plasma during the helicon mode of the discharge. The strong dependence of the plasma current on the helicon mode of the discharge has been observed during the present experimental study.

---

## 1. Introduction

Helicon waves are considered good sources of high-density plasma with high ionization efficiency and, hence, they are of common interest for plasma processing [1], in-space thrusters, space-relevant experiments [2] and wave-physics experiments [3]. The capability of a helicon wave to drive current in a plasma has been scarcely explored experimentally. Toroidal magnetic confinement experiments require electrical current in the plasma in order to generate rotational transform along with better particle confinement. Current drive in a toroidal plasma column is possible when there is a large tail in one direction in the electron distribution function, a drifting distribution or both [4]. Wave-particle resonance, better known as Landau damping which leads to the former methodology of current drive, dominated the study of current drive by helicon waves during the investigations reported earlier [5–7]. Non-resonant current drive by the dynamo field components of helicon waves has been investigated [8, 9] through experiments and numerical estimations. A strong poloidal asymmetry in the wave magnetic field components, measured across the radius, during helicon discharge in a small aspect ratio torus, is responsible for a significant current drive through wave-induced helicity [8]. Quantitative comparisons of common current drive theory with helicon current drive have been performed by Tripathi and Bora [5], later elaborated by Paul and Bora [8] for non-resonant current drive by helicon waves. These recent reports suggest that the poloidal asymmetry in the wave magnetic field components needs further investigation.

<sup>†</sup> Present address: IEF-4, Forschungszentrum Julich GmbH, D-52425 Juelich, Germany.

In this paper we report on the evolution of poloidal asymmetry in the wave magnetic field components during discharge mode transitions. The rise in the magnitude of the radial electric field with radiofrequency (RF) power, observed during discharge mode transition, support better radial confinement of the plasma during the helicon mode of the discharge. The dependence of plasma current on the mode of discharge is also presented.

## 2. Setup and diagnostics

The Toroidal Helicon Plasma Device (THPD) has been described previously [10] and consists of a toroidal vacuum chamber of 10.5 cm minor radius and 30 cm major radius. The system is pumped down to a base pressure of  $1 \times 10^{-5}$  mbar using two diffusion pumps and backed by a rotary pump, connected at toroidal locations  $180^\circ$  apart. The toroidal magnetic field in this system is produced by four sets of magnetic field coils, wound on each quadrants of the toroidal vacuum vessel. The only source to produce plasma in THPD is a right helical antenna, placed inside the vacuum chamber, electrically isolated from plasma. It is essentially used to excite the  $m = +1$  mode of helicon waves. During this study, the coils are fed a pulsed current of 1.8 kA (peak) and the toroidal magnetic field ( $B_T$ ) of 1 kGauss (peak) is generated for 50 ms (full width at half maxima), requisite to excite the helicon waves. The argon pressure is maintained in the range  $(5-2) \times 10^{-3}$  mbar. The source is fed from a  $L$ -type impedance matching network/generator system operating at 32 MHz. During the experiments, at the desired fill pressure of argon gas, the pulsed magnetic field triggers the discharge for 50 ms, via efficient wave coupling. The plasma is diagnosed by a RF compensated Langmuir probe [11], tri-axial center-tapped B-dot (magnetic loop) probes with bifilar turns, placed toroidally next to the antenna to observe radial variation of plasma parameters. A dual Rogowski coil system, encircling the entire plasma cross section, is used to measure the average plasma current [12]. All of the diagnostics are mounted in radial ports at  $50^\circ$  inclination from the equatorial plane, on both sides of the helical antenna. The Rogowski coil system is introduced radially into the toroidal vacuum chamber, toroidally opposite to the helical antenna, with the major opening of coil housing encircling the plasma cross section. Axial and poloidal array of B-dot probes are also used to measure the spatial variations of radial ( $r$ ), azimuthal ( $\theta$ ) and toroidal ( $\phi$ ) wave magnetic field components ( $B_{r,\theta,\phi}$ ). Although analogous study is also possible by many advanced techniques, the simplicity and wide variety of magnetic loop probe diagnostics [13] available still remain unmatched. Measurements were repeated at different toroidal and poloidal locations so as to cover maximum number of nodal points on the poloidal plane.

Variation of density with input RF power, at  $B_T \approx 0.5$  kGauss, measured by a RF compensated Langmuir probe, is plotted in Fig. 1. With increasing RF power, the discharge snaps from the inductive mode to the helicon mode, as suggested by the radial profile of density measured during the inductive mode and helicon mode of discharges [10, 11], as plotted in Fig. 2. A typical peaked radial density profile, measured during the helicon mode of the discharge, suggests enhanced ionization coupled with better radial confinement of electrons. To comprehend the evolution of helicon wave sustained discharge with increasing input RF power,  $B_{r,\theta,\phi}$  components were measured during progressively increasing density levels. The computed wave magnetic field profiles of  $m = +1$  helicon mode of discharge

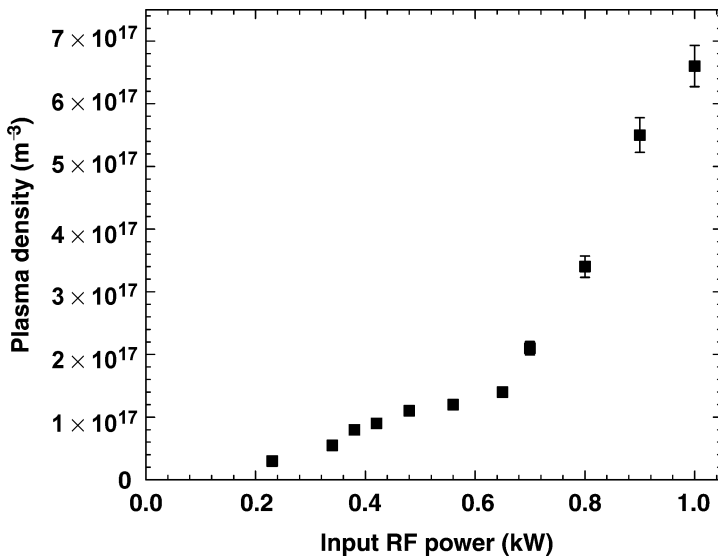


**Figure 1.** Variation of plasma density  $n_e$  with RF power, at  $B_T \approx 0.5$  kGauss, during helicon discharge, clearly reveals the discharge mode transitions at (0.4–0.5) kW and (0.6–0.7) kW.

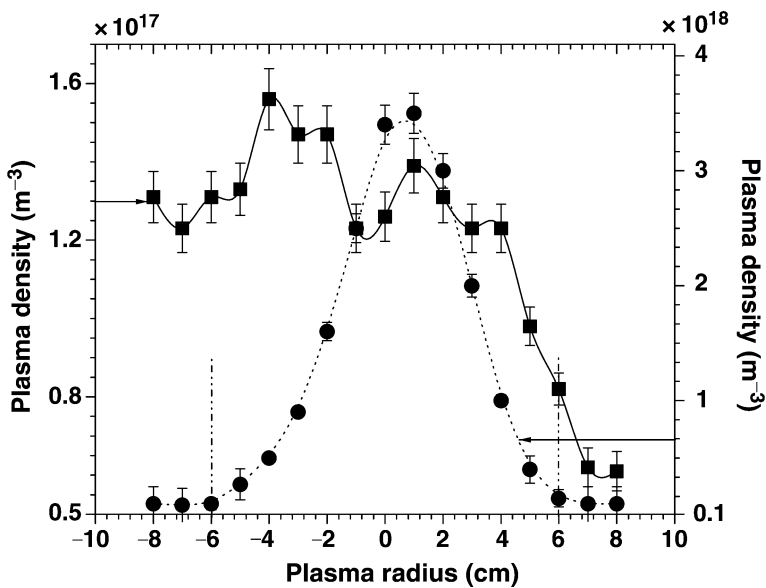


**Figure 2.** Radial profiles of plasma density measured during the inductive mode and the helicon mode of the discharge at  $P_{\text{rf}} \approx 0.5$  kW,  $B_T \approx 0.5$  kGauss and  $P_{\text{rf}} \approx 1.4$  kW,  $B_T \approx 0.8$  kGauss, respectively. The vertical lines at  $\pm 6$  cm correspond to the antenna aperture.

in THPD have been estimated on the basis of a toroidal model [8, 14]. The  $B_{r,\theta,\phi}$  components measured in plasma density ( $n_e \approx 10^{17} \text{ m}^{-3}$ ), input RF power ( $P_{\text{rf}} \approx 600$  W) and ( $B_T \approx 0.4$  kGauss), are shown in Fig. 3. During  $B_{r,\theta,\phi}$  measurement, the three-dimensional probe set was moved from the outboard to the inboard direction, passing through the plasma center. The radial density profile measured

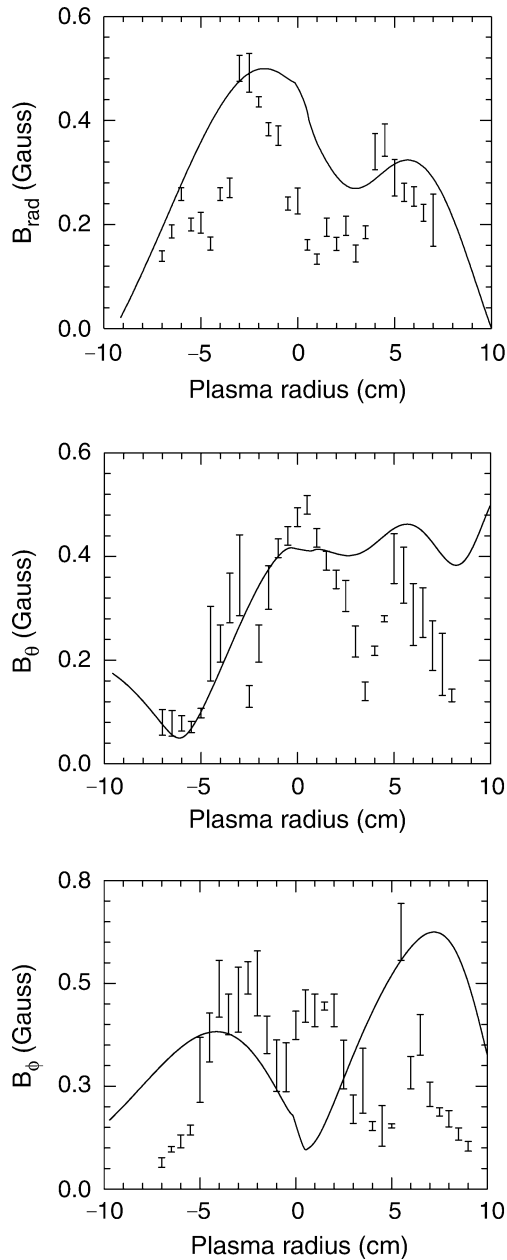


**Figure 3.** Radial profiles of radial ( $r$ ), azimuthal ( $\theta$ ) and toroidal ( $\phi$ ) wave magnetic field components measured during inductive mode of discharge, at  $n_e = 10^{17} \text{ m}^{-3}$ ,  $P_{\text{rf}} = 0.5 \text{ kW}$  and  $B_T = 0.5 \text{ kGauss}$ . Solid lines indicate the computed profiles in arbitrary units and the bars indicate the measured values in Gauss. Increasing values on the horizontal axis indicate the probe positions from inboard to outboard.

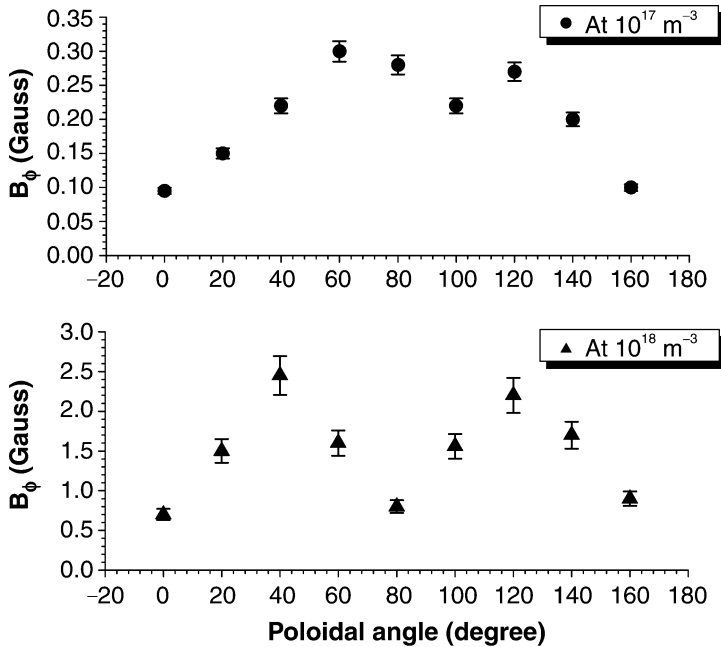


**Figure 4.** Poloidal variation of the toroidal ( $\phi$ ) component of wave magnetic field ( $\partial B_\phi / \partial \theta$ ), measured during inductive and helicon modes of discharges.

in this parameter regime, shown in Fig. 2, suggests that the mode of discharge is essentially inductive [10]. A prominent difference could be observed between the  $B_{r,\theta,\phi}$  components measured during the inductive mode of the discharge and the computed spatial profiles of  $B_{r,\theta,\phi}$  components for helicon discharge in THPD, as expected. The wave magnetic field components measured during the inductive mode of the discharge in THPD are compared with those computed for the helicon mode of the discharge in THPD to point at the conspicuous evolution of spatial  $B_{r,\theta,\phi}$  structures.

### 3. Radial characterization of wave magnetic field components

The inductive to helicon mode transition has been observed at  $P_{\text{rf}} \approx 700$  W and  $B_T \approx 0.5$  kGauss. During the helicon wave sustained discharge mode, resistivity increases owing to collisional effects (in the high-pressure regime) [8] and other non-resonant wave-particle interactions [15]. The increasing resistivity further enhances the penetration of the  $B_\phi$  component hence providing a positive feedback which is consistent with the apparent change of mode. Poloidal variation of the  $B_\phi$  component of the wave magnetic field is measured using a poloidal array of B-dot probes, placed 20 cm away from the antenna, along the toroidal magnetic field direction, shown in Fig. 4. Measurements of variations of  $B_{r,\theta,\phi}$  components in two different discharge regimes were made. A comparison of poloidal variation of  $B_\phi$  during the inductive mode of discharge ( $n_e = 10^{17} \text{ m}^{-3}$ ) and helicon wave sustained discharge ( $n_e = 10^{18} \text{ m}^{-3}$ ) are shown in Fig. 4. Increasing magnitudes of

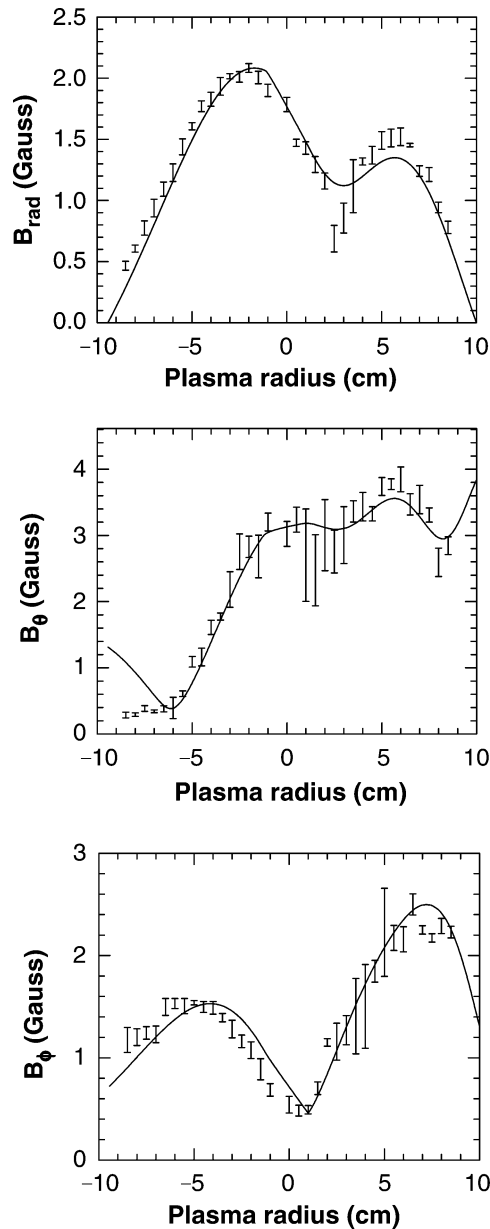


**Figure 5.** Radial profiles of  $B_{r,\theta,\phi}$  components measured during helicon discharge, at  $n_e = 10^{18} \text{ m}^{-3}$ ,  $P_{\text{rf}} = 1.4 \text{ kW}$  and  $B_T = 0.8 \text{ kGauss}$ . Solid lines indicate the computed profiles in arbitrary units and the bars indicate the measured values in Gauss. Increasing values on the horizontal axis indicate the probe positions from inboard to outboard.

spatial  $B_{r,\theta,\phi}$  envelopes and poloidal asymmetry, measured in the parameter regime of helicon discharge, are indicative of the energy gained by the helicon wave which further enhances the density.

During high-power helicon discharge ( $n_e \geq 10^{12} \text{ m}^{-3}$ ,  $P_{\text{rf}} \geq 1.2 \text{ kW}$  and  $B_T \geq 0.7 \text{ kGauss}$ ) the measured radial structures of  $B_{r,\theta,\phi}$  components are shown in Fig. 5.

The measured profiles are in good agreement with the computed profiles for helicon discharge in THPD. Spatial magnetic field measurements were made at the same poloidal angle as that considered for the computation. Larger error bars on the  $B_{r,\theta,\phi}$  profiles, on the outboard side, indicate fluctuation in the magnitudes of wave magnetic field components owing to large variation of toroidal magnetic field. The increase in poloidal asymmetry and magnitudes of radial profiles of  $B_{r,\theta,\phi}$  components, measured during helicon mode of discharge, is observed. Multiple peaks in the measured  $B_r$  component of the wave magnetic field suggest successful helicon discharges of  $m = \pm 1$  azimuthal modes [16]. However, the  $m = -1$  mode cannot be excited in THPD using the right helical antenna, under present experimental conditions [10]. A significant increase in the magnitude of the  $B_\theta$  component, as evident from Figs 3 and 5, suggests an increase in the radial component of the wave electric field [17], which supports better radial confinement of plasma, as suggested by the radial profiles of density plotted in Fig. 2 (see [8]). The difference between the magnitudes of  $B_r$  and  $B_\theta$  envelopes suggest that the wave excited in the present parameter regime might be elliptically polarized. The spatial asymmetry in the radial profiles of  $B_{r,\theta,\phi}$  components measured during the inductive mode of the discharge suggests that although helicon waves can be excited during the inductive mode of the discharge, the impact of wave magnetic field structures (imposed by the antenna) on the plasma is negligible. Multiple maxima in the radial profile of the radial component of the wave magnetic field ( $B_r$ ) measured during helicon discharge, shown in Fig. 5, suggest that tight boundary conditions and toroidicity in  $B_T$  (resulting inhomogeneity) have a significant influence on the wave magnetic field profiles [10]. The possible involvement of higher radial or azimuthal modes needs further attention which is beyond the scope of the present discussion [14].

#### 4. Current drive during helicon mode of discharge

A dual Rogowski coil system is used to measure the plasma current generated during helicon discharge in THPD [12]. Concomitant reversal of the plasma current with  $B_T$  and antenna polarity ensures proper and genuine measurement of average plasma current in THPD [8]. Variation of the plasma current with  $B_T$  in two different density regimes,  $7 \times 10^{17} \text{ m}^{-3}$  and  $2 \times 10^{18} \text{ m}^{-3}$ , during helicon discharge in THPD are plotted in Fig. 6. An abrupt jump in the magnitude of plasma current could be observed due to mode transition during low-power experiments in THPD. Variation of the plasma current follows the trend observed for density, as shown in Fig. 1, which suggests a strong dependence of the plasma current on the helicon mode of discharge. During the low-power current drive experiments, the RF power followed the toroidal magnetic field, with a suitable delay time, so that the jump in current signal, owing to discharge mode transition, could be prominently observed during the decay phase of plasma current. The fast ramp up of plasma current ( $I_P$ ) during high-power helicon discharges, is evident in the typical temporal profile of the measured average plasma current in THPD, as shown in Fig. 7. High-power current drive experiments were initiated by RF power followed by the toroidal magnetic field. However, it should be noted that discharge mode transition varies with the magnitudes of  $B_T$  and input RF power. Proper isolation between different ground schemes is used to avoid any ground loop and minimize the unbalance currents. To substantiate the absence of pick-up due to

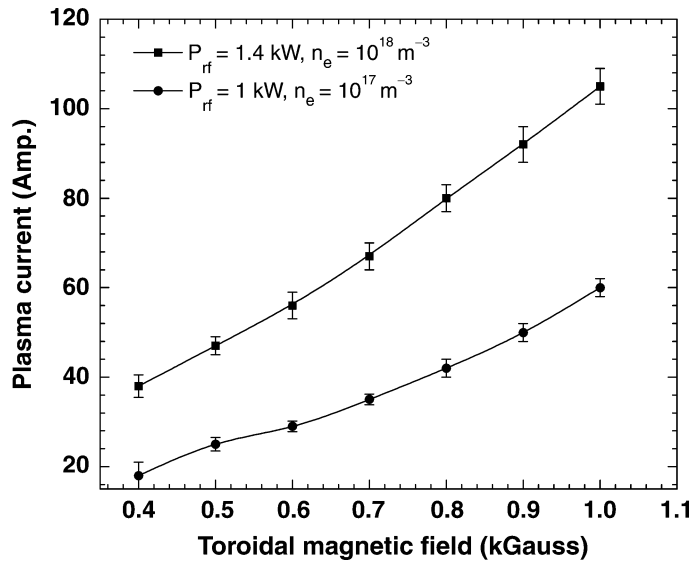


**Figure 6.** Variation of the plasma current with toroidal magnetic field, during helicon discharges at input RF power  $P_{rf} = 1 \text{ kW}$  and  $P_{rf} = 1.4 \text{ kW}$ .

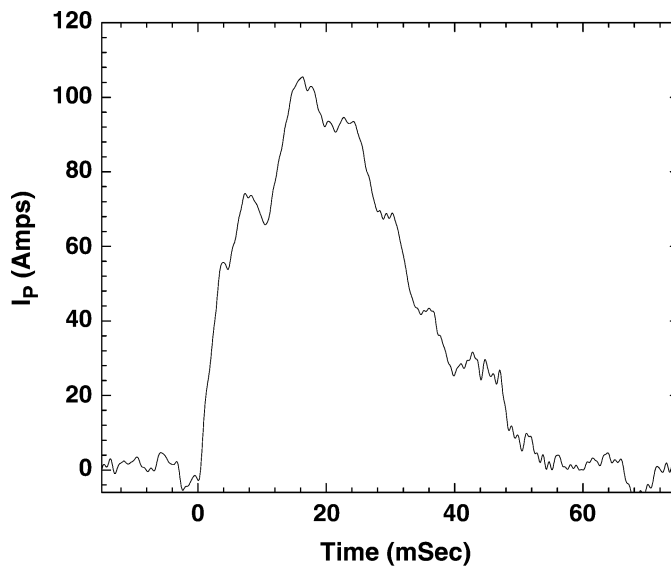


**Figure 7.** Typical temporal profile of plasma current measured during high-power helicon discharge at an input RF power 1.4 kW and ambient magnetic field 0.9 kGauss.

any closed loop of current formed inside THPD, measurements of plasma current were made at different toroidal locations. In the absence of sufficient energetic non-thermal plasma constituents during our experimental investigation, performed in the very-high-frequency operational regime, ponderomotive sources [ $J \times B$ ] are



mainly responsible for the current drive observed during the helicon mode of the discharge in THPD [18].

## 5. Conclusion

The radial measurements of the wave magnetic field components made during discharge mode transition, from the inductive mode to the helicon mode of the discharge, clearly show the evolution of strong poloidal asymmetry in the spatial  $B_{r,\theta,\phi}$  structures which contribute to the wave-induced helicity during the helicon mode of the discharge. The increase in the magnitude of the radial wave electric field supports better radial confinement and contributes to the wave-induced helicity during the helicon mode of the discharge. The wave-induced helicity could be the reason for the higher plasma current observed during the helicon mode of the discharge. The current drive experiments, discussed here, also suggest a connection between the plasma current and the helicon mode of the discharge in THPD.

## References

- [1] Chavers, D. G., Chang-Diaz, F. R., Irvine, C. and Squire, J. P. 2006 Momentum and heat flux measurements using an impact target in flowing plasma. *J. Propulsion Power* **22**, 637–644.
- [2] Scime, E. E., Keiter, P. A., Zintl, M. W., Balkey, M. M., Kline, J. L. and Koepke, M. E. 1998 Control of ion temperature anisotropy in a helicon plasma. *Plasma Sources Sci. Technol.* **7**, 186–191.
- [3] Krämer, M., Aliev, M. Yu., Altukhov, A. B., Gurchenko, A. D., Gusakov, E. Z. and Niemi, K. 2007 Anomalous helicon wave absorption and parametric excitation of electrostatic fluctuations in a helicon-produced plasma. *Plasma Phys. Control. Fusion* **49**, A167–A175.
- [4] Fisch, N. J. 1987 Theory of current drive in plasmas. *Rev. Mod. Phys.* **59**, 175.
- [5] Tripathi, S. K. P. and Bora, D. 2002 Current drive by toroidally bounded whistlers. *Nucl. Fusion* **42**, L15.
- [6] Takamura, S., Kojima, T. and Okuda, T. 1983 Radio Frequency current generation by helical slow-wave antennas in a torus. *Plasma Phys.* **25**, 1469–1482.
- [7] Zhang, B. C., Blackwell, B. D., Borg, G. G. and Petřížilka, V. 1997 Observation of the neoclassical current in the Small Helic Experimental Apparatus (SHEILA). *Phys. Plasmas* **4**(11), 3986.
- [8] Paul, M. K. and Bora, D. 2007 Wave-induced helicity current drive by helicon waves. *Phys. Plasmas* **14**, 082507.
- [9] Scime, E. E., Keese, A. M. and Boswell, R. W. 2008 Mini-conference on helicon plasma sources. *Phys. Plasmas* **15**, 058301.
- [10] Paul, M. K. and Bora, D. 2005 Helicon plasma production in a torus at very high frequency. *Phys. Plasmas* **12**, 062510.
- [11] Paul, M. K. and Bora, D. 2008 Langmuir probe study in the nonresonant current drive regime of helicon discharge. *Pramana* **71**(1), 117.
- [12] Paul, M. K., Chattopadhyay, P. K. and Bora, D. 2007 Electrostatic pickup rejection in low plasma current measurement. *Meas. Sci. Technol.* **18**, 117.
- [13] Franck, C. M., Grulke, O. and Klinger, T. 2002 Magnetic fluctuation probe design and capacitive pickup rejection. *Rev. Sci. Instrum.* **73**(11), 3768.
- [14] Tripathi, S. K. P. and Bora, D. 2001 Normal modes of bounded whistler produced toroidal plasmas. *Phys. Plasmas* **8**, 697.

- [15] Blackwell, D. D., Madziwa, T. G., Arnush, D. and Chen, F. F. 2002 Evidence for Trivelpiece–Gould modes in a helicon discharge. *Phys. Rev. Lett.* **88**, 145002.
- [16] Light, M. and Chen, F. F. 1995 Helicon wave excitation with helical antennas. *Phys. Plasmas* **2**, 1084.
- [17] Chen, F. F. 1991 Plasma ionization by helicon waves. *Plasma Phys. Control. Fusion* **33**, 339.
- [18] Paul, M. K. and Bora, D. 2009 Current drive by helicon waves. *J. Appl. Phys.* **105**, 013305.